Depth-enhanced integral-imaging 3D display using different optical path lengths by polarization devices or mirror barrier array

Sungyong Jung
Jisoo Hong
Jae-Hyeung Park
Yunhee Kim
Byoungho Lee

Abstract — Depth-enhanced integral three-dimensional (3D) imaging using different optical path lengths by using a polarization selective mirror pair or mirror barrier array is proposed. In the proposed approach, the enhancement of image depth is achieved by repositioning two types of elemental image planes, thus effectively two central depth planes are obtained. One of the two implementation methods makes use of the two-arm structure that has different optical path lengths and polarization-selective mirrors. The other utilizes the mirror barrier array. The primary advantage of the method with polarization devices is that we can observe 3D images that maintain some level of viewing resolution with a large depth difference without any mechanical moving part. The mirror barrier array has the advantage of the compact thickness. We demonstrated and verified our proposals experimentally.

Keywords — *Three-dimensional display, integral imaging, depth enhancement, optical path control.*

1 Introduction

Integral imaging (InIm) has attracted much attention recently due to its outstanding advantages over other three-dimensional (3D) display technologies.[1–3] First of all, InIm is an autostereoscopic method, which means that it does not require any special viewing aids to see 3D images. In addition, InIm provides continuous viewpoints within specific viewing angle. Unlike the conventional stereoscopic method based on a lenticular lens, it also has full parallax along both the horizontal and vertical directions. The major drawback of InIm in early times was the limitation of implementing dynamic 3D images. The use of passive devices as recording and displaying media prevented integrating 3D images in real time. With the rapid development of active devices, CCDs (charge coupled devices) and flat-panel displays have substituted for the film recently, and subsequently real-time implementation of 3D displays based on InIm became possible. The configuration of the real-time InIm is shown in Fig. 1. However, there still remain several problems, including pseudoscopic images, limitation of viewing angle, and resolution degradation, that should be overcome. Continuous studies have been performed to improve such problems.[4–10]

Along with those problems mentioned above, the limitation of image depth is another main bottleneck of integral imaging. The objective of InIm is to display a 3D object that has some thickness along the depth direction. Hence, the effort to increase the image depth for the display of 3D objects is indispensable. The limitation of image depth should be considered with the limitation of viewing resolution of the integrated image. In InIm, the quality of the reconstructed image is best at the central depth plane (the focused image plane where the center of an object is positioned), and it becomes worse at the marginal planes (the defocused end planes out of the central depth plane). Consequently, there exists a finite depth range within which some level of viewing resolution is maintained. Figure 2(a) shows the geometry of the limited depth range. The main cause that degrades the resolution at a position out of the central depth plane is image blurring (or smearing) as the graphs in Fig. 2(b) illustrate. As the image plane gets more defocused, the intensity profile spreads more along the lateral direction. This can also be thought as a problem caused by limited depth of focus in each elemental lens. Detailed theoretical analysis on the depth-limitation and resolution degradation is given in Ref. 11.

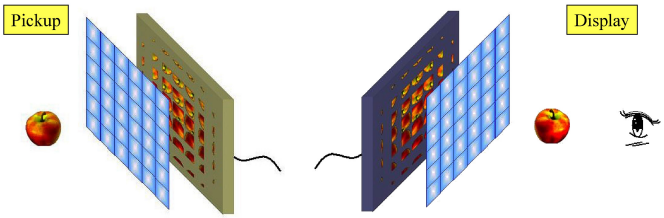


FIGURE 1 — Basic concept of InIm.

Because the implementable depth is an important issue in InIm, a major part of research on InIm was how to enhance the depth limitation. As a result of such efforts, many schemes that showed impressive enhancement on the depth limitation were proposed. One of early works is to change the gap between the display panel and the lens array by moving the lens array on the motorized stage in the direction perpendicular to the display panel.[12] Then the location of the central depth plane can be changed to express wider range in the direction perpendicular to the display panel. However, this method demands high-speed movement of the lens array, and it raises the problem of system reliability. Multiple central depth planes also can be obtained

Revised version of a paper presented at the 8th Asian Symposium on Information Display held February 14–17, 2004, in Nanjing, China.
The authors are with the National Research Laboratory of Holography Technologies, School of Electrical Engineering, Seoul National University, Seoul 151-744, Korea; telephone +82-2-880-7245, fax +82-2-873-9953, e-mail: byoungho@snu.ac.kr.
© Copyright 2004 Society for Information Display 1071-0922/04/1204-0000461$1.00

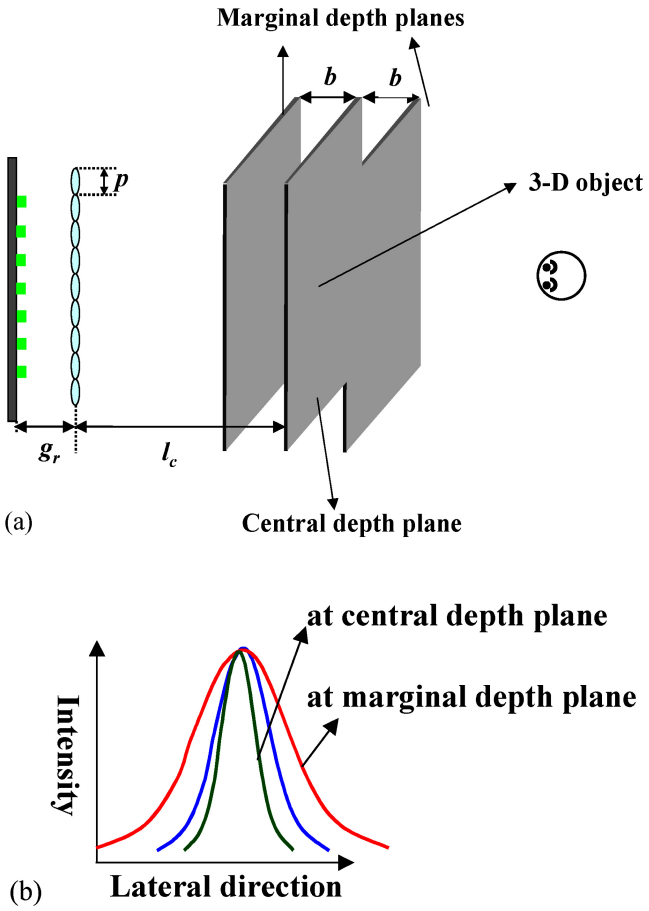


FIGURE 2 — Depth limitation of InIm. (a) Geometry of the limited depth range. (b) The image blurring (or smearing) at the central or marginal depth plane.

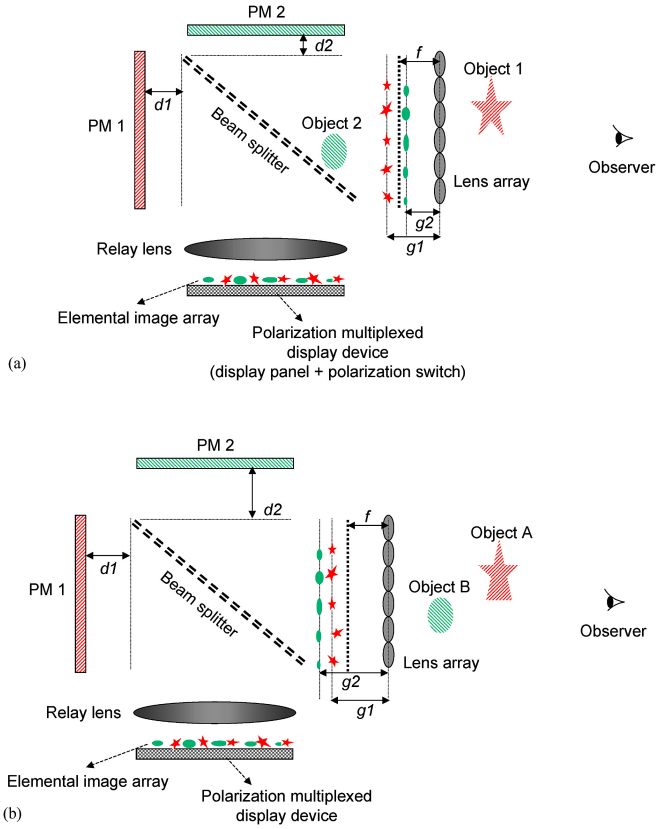


FIGURE 3 — System configuration of the proposed scheme. (a) Utilizing RII and VII, (b) utilizing only RII.

by adopting two InIm systems.[13] The gaps of each system are set to different values, so each system has a different central depth plane. Two systems are combined with a beam splitter, and then two different central depth planes generated by each system can be implemented simultaneously. However, aligning the system is very difficult and the size of the system becomes very bulky. Another scheme is to use a uniaxial crystal plate and an LCD shutter to produce triple central depth planes.[14] The problems of this scheme are the demand of a very fast device and the limited quality of integrated images.

In this paper, we propose a novel technique to increase the range of image depth in integral 3D imaging systems by use of different optical path lengths with polarization-selective mirrors or the mirror barrier array. The proposed scheme with polarization-selective mirrors is based on the scheme of double display devices, but the structure is relatively compact because we require only one lens array and one display device. The scheme with the mirror barrier array is more compact but it demands mechanical motion. For simplicity, it is assumed that the elemental images are generated by computer graphics, not by pickup process. The enhancement of image depth is achieved by repositioning two types of elemental image planes simultaneously by adopting additional structure to the conventional scheme, thus effectively two central depth planes are obtained. The proposed system makes use of a two-arm structure that has polarization-selective mirrors or the mirror barrier array to utilize different optical path lengths. The configuration of the proposed system with the polarization-selective mirrors is shown in Fig. 3.

2 System configuration of two-arm structure using polarization-selective mirror pair

Basically, we utilized multiplexed image planes that have different central depth planes so that we could increase the image-depth range. The input field that contains the information of elemental images is illuminated from the polarization-multiplexed display device. The polarization- multiplexed display, which displays multiplexed signals in synchronization with the polarization switching, is a commercially available product because it is widely used in the field of stereoscopic displays.

The input beam is relayed through a relay lens and divided into two beams by a beam splitter. Then each beam is reflected by mirrors, recombined by a beam splitter, and passes through a lens array. The noticeable point here is that beams in two arms undergo different path lengths due to the unequal distances between the mirrors and the beam splitter. We can control the distances arbitrarily for our pur-

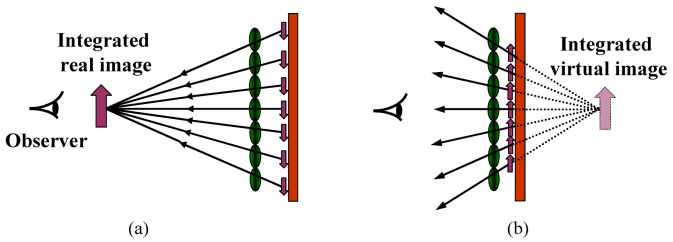


FIGURE 4 — (a) Real and (b) virtual integrated images.

poses. Another distinct feature of this system is that we use polarization-selective mirrors which reflect a particularly polarized beam selectively. Hence, if each mirror in two arms reflects only horizontal or vertical polarization selectively, for example, and if the polarization switcher provides both horizontal and vertical polarizations with time multiplexing, the beams that are reflected by the mirrors in the two arms contain polarization components that are orthogonal to each other. These polarized beams form images of relay lens at different positions because the optical path lengths in two arms are different. In this scheme, the optical path lengths in two arms are controlled by adjusting the distances d_1 and d_2 (see Fig. 3) so that the relation, $g_1 - g_2 = 2(d_1 - d_2)$, is satisfied, *i.e.*, the distance difference between g_1 and g_2 corresponds to the double of the difference between d_1 and d_2. Subsequently, the gap between the lens array and elemental images is different for each polarized beam. This leads to the creation of two central depth planes according to the corresponding gaps. Moreover, if we adjust the distances d_1 and d_2 properly, the position of the integrated images can be controlled. So both the real integral imaging (RII) and virtual integral imaging (VII) can be applicable in this scheme. If we adjust the distance between the lens array and the display panel to be larger than the focal length of the elemental lenses, the central depth plane is located in front of the lens array. In this case, the integrated image can be reconstructed as a real image in front of the lens array as shown in Fig. 4(a) and it is called RII.[11,12] On the other hand, if the distance between the lens array and the display panel is shorter than the focal length, the hypothetical central depth plane is formed behind the lens array. In this case, the integrated image is reconstructed as the virtual image as shown in Fig. 4(b), and it is called VII.[11,12] For example, if we adjust the distance d_1 and d_2 so that the focal length of elemental lenses is shorter than g_1 and longer than g_2 as in Fig. 3(a), the real (Object 1) and virtual (Object 2) images are reconstructed in front of and behind the lens array, respectively. As a result, the observer can see 3D real and virtual images with large depth difference simultaneously if we assume that the polarization switching is fast enough to prevent image flickering. If we adjust the distance d_1 and d_2 so that the focal length of an elemental lens is shorter than g_1 and g_2 (g_2 is larger than g_1) as in Fig. 3(b), two real images (Object A and Object B) are reconstructed in front of the lens array. In this case, the image depth of Object A is greater than that of Object B. Although the depth difference between the Object A and

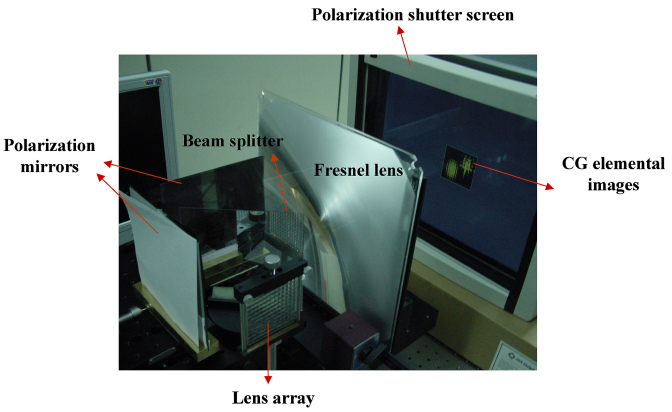


FIGURE 5 — Experimental setup for the two-arm structure.

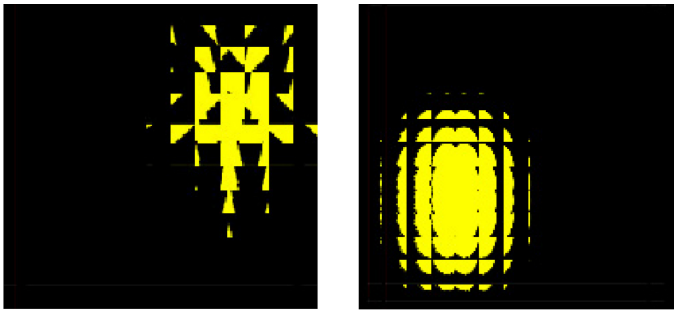
Object B is reduced than the case of Fig. 3(a), the range of image depth is still much increased because we have two central depth planes for both objects. Similarly, if we adjust the distances d_1 and d_2 so that both arms operate in the VII mode, then virtual images with different depths are simultaneously obtainable.

3 Experimental results for the two-arm structure

Of course, in our proposal, the simultaneous implementation of both real images or that of both virtual images is also possible through a proper control of distances d_1 and d_2. However, to fully utilize the feeling of depth difference, we demonstrated the feasibility of the scheme in Fig. 3(a) experimentally, and thus realized simultaneous display of real and virtual images. The target image depths of real and virtual images were 70 and –70 mm from the lens array, respectively. (The minus sign denotes that the integrated image plane is located behind the lens array.)

TABLE 1 — Specifications of the equipments used in the experiment.

Setup	Specification	Values
Display panel (21-in. flat-panel CRT)	Number of pixels	1024(H) ×768(V)
	Pixel size	0.36 mm
Lens array	Number of elemental lenses	13(H) ×13(V)
	Pitch of the elemental lens	5 mm
	Focal length	30 mm
Polarization shutter screen	Type of polarization	Linear (horizontal & vertical)
	Stereoscopic field rate	120 Hz
Relay lens (Fresnel lens)	Focal length	170 mm
	Size (diagonal)	21-in.
Polarization selective mirrors	Type of polarization	Linear (horizontal & vertical)

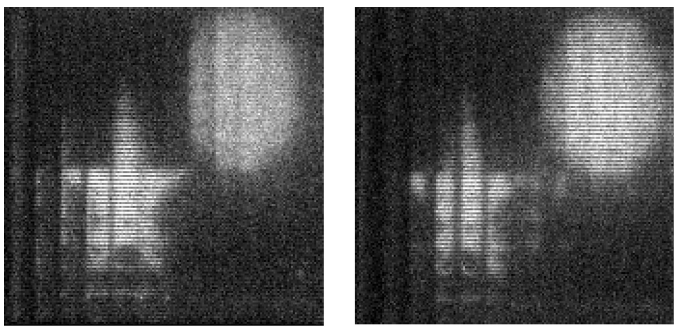


(a) (b)

FIGURE 6 — Elemental images for the experiment. (a) For RII and (b) VII.

The values of g_1 and g_2 for these locations of central depth planes correspond to 52 and 21 mm, respectively. The characteristics of the used lens array are presented in Table 1. As we can see from the figure, if the gap changes due to the path length difference in two arms by a few centimeters, both real and virtual images can be displayed, *i.e.*, the image depth difference can be selected by controlling the difference in the gaps. For example, the gap difference of 31 mm leads to the image position difference of 140 mm in the figure. Figure 5 shows the implemented system following the specifications discussed above.

Figures 6(a) and (b) show computer-generated elemental images for real and virtual objects, respectively. These two types of elemental image arrays are displayed on a flat-panel cathode-ray-tube (CRT) display (pixel pitch: 0.36 mm) and encoded by one of the two orthogonal polarizations after passing through the polarization shutter screen (polarization switcher). The stereoscopic field rate that represents the polarization switching speed is 120 Hz, which is a flicker-free frequency. The polarization states of both polarization switcher and polarization-selective mirrors are linear – the horizontal and the vertical polarizations. Then, polarization-multiplexed elemental image arrays are repositioned through a Fresnel lens with a focal length of 170 mm, which plays a role of relaying the elemental images from the display to the position around the lens array. Both mirrors in two arms are attached to translation stages controlled by micrometers, and the distance difference between d_1 and d_2 was set to 15.5 mm in order to obtain a gap difference of 31 mm. The lens array used in this experiment consists of 13×13 square elemental lenses that have a pitch of 5 mm and a focal length of 30 mm. Figure 7 shows integrated images that are observed from different viewing directions. As the figure shows, we could successfully reconstruct real and virtual images with depth difference of 140 mm at once. The horizontal parallax can be seen (the shape and relative separation in the captured two images are slightly different according to the viewing position). Unfortunately, the amount of parallax is not so much in our preliminary experiments because the viewing range is restricted into a small region. This is because the viewing angle of this system is small (less than 3° in one side) due to the fact that the used lens array has a large *f*-number (it is well known that the viewing angle in InIm is inversely proportional to the *f*-number of elemental lenses[11]). However, we expect that larger amount of parallax can be achieved if we adopt a lens array with a smaller *f*-number.



(a) (b)

FIGURE 7 — Experimental results.

4 Mirror barrier array

The principles of the proposed method based on the mirror barrier array are shown in Fig. 8. The mirror barrier array is composed of many elemental mirrors that are located between lens array and the display panel and each elemental mirror is laid to separate each column of elemental lenses. Initially, elemental mirrors are perpendicular to the lens array as shown in Fig. 8(a), so the observer in a certain viewing angle cannot realize the existence of mirrors. In that state, the elemental images are integrated by the lens array at the central depth plane 1 whose location is determined simply by the gap g between the lens array and the display panel. Then the mirrors (both-sides reflection mirrors) change their poses to make an angle of 45° with the lens array as shown in Fig. 8(b). In that state, the elemental images displayed by the display panel are reflected between adjacent mirrors, and they go through increased optical path length. Then the central depth plane 2 is formed at a different location from that of the central depth plane 1 of the initial state. Its location d_2 is determined by the optical path length made by adding the gap g (between the lens array and the display panel) and the pitch of the elemental lens φ that is pertinent to the path length difference made by reflections between mirrors. By switching between these two states rapidly, we can obtain two central depth planes simultaneously. Considering the simple lens law, the location of the central depth plane is inversely proportional to the optical path length that the elemental image goes through before it meets the lens array. Therefore the initial state of the mirror barrier array generates the central depth plane farther from the lens array than the state where mirrors are inclined does. Each state takes charge of a certain expressible thickness of the integrated image, so we should design the various optical parameters of the system to cascade each expressible thickness properly.

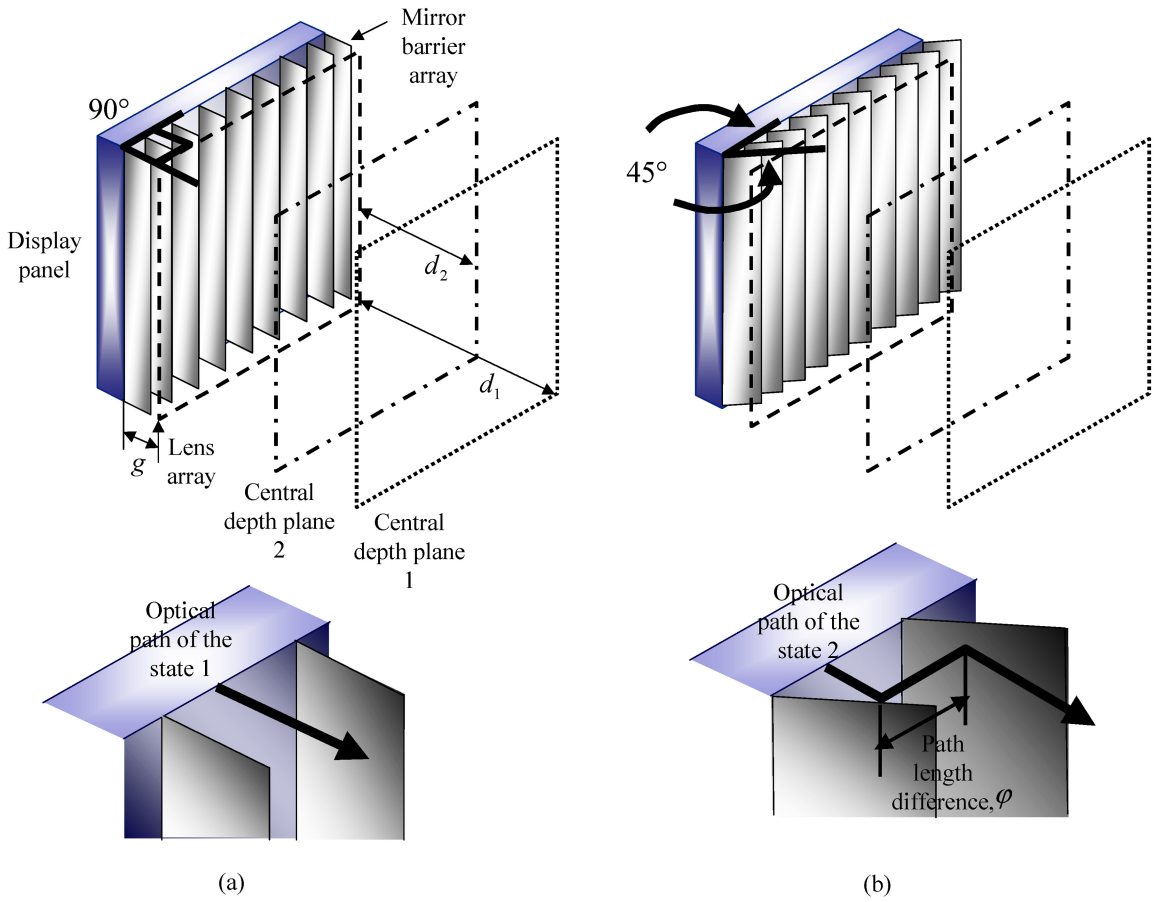


FIGURE 8 — System configuration of the proposed scheme. (a) Perpendicular-mirror state (State 1). (b) Tilted-mirror state (State 2).

We performed the experiments to display the integrated images around two central depth planes with the system assembled based on the proposed method described above. In the experiment, we used the mirror barrier array whose states can be changed manually to verify that the integrated images are formed around two central depth planes. Each elemental mirror that composes the mirror barrier array has the length of 14 mm in the horizontal direction, 130 mm in the vertical direction, and a thickness of 2 mm. The dimensions of the elemental mirror had been determined to correspond to the other components, especially the lens array. The lens array is composed of 13 elemental lenses in both of the horizontal and vertical directions. The pitch of the elemental mirror φ is 10 mm, and the focal length is 22 mm. Considering the state 2 of the mirror barrier array, the length of the elemental mirror in the horizontal direction should be $\sqrt{2}\varphi$ as the elemental mirrors are inclined with an angle of 45° in that state. However, the exact value is an irrational number, so we determined that as 14 mm. There exist some errors in the range of 2–3 mm in the dimension of the elemental mirrors and such errors do not affect the results of the experiment significantly. The gap g was determined to be 25 mm, so the distance d_1 of the target central depth plane 1 in the state 1 from the lens array becomes 183 mm. Then the effective gap between the lens array and the display panel in the state 2 becomes $g + \varphi$, or 35 mm, forming the target central depth plane 2 at the location of 59 mm from the lens array. Therefore, the display panel in the state 1 should display the elemental images that are integrated around the central depth plane 1, and the elemental images of the integrated image around the central depth plane 2 should be displayed in the state 2. These two elemental images are displayed on the LCD with the pixel pitch of 0.31 mm in the horizontal direction and 0.32 mm in the vertical direction. All the ele-

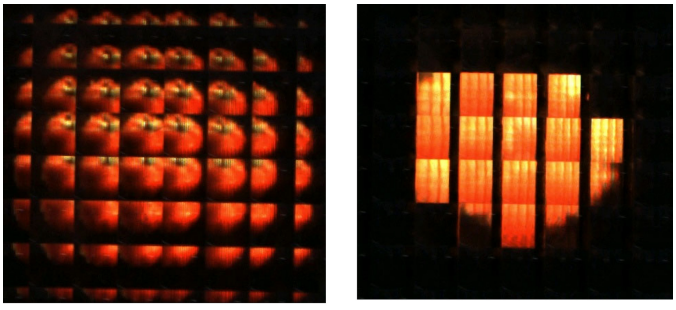
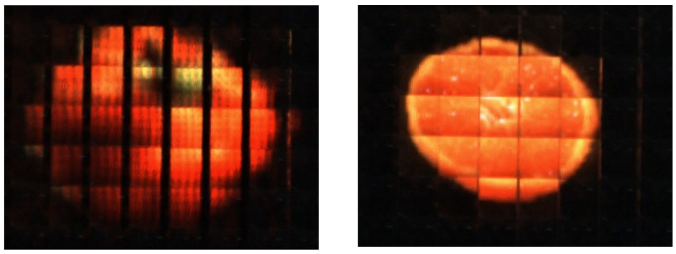


FIGURE 9 — Integrated images displayed out of the central depth plane. (a) Image at 183 mm and central depth plane at 59 mm. (b) Image at 59 mm and central depth plane at 183 mm.



(a) (b)

FIGURE 10 — Integrated images displayed by proposed method. (a) State 1 of mirror barrier array. (b) State 2 of mirror barrier array.

mental images used in the experiments are generated by the computer graphics.

We performed a preliminary experiment for the comparison of the conventional and the proposed scheme as shown in Figs. 9(a) and (b). The experiment shows how the quality of the integrated image degrades when the integrated image is located out of the central depth plane. In Fig. 9(a), the integrated image is located at 183 mm from the lens array and the gap g is set to 35 mm to locate the central depth plane at 59 mm distance from the lens array. As shown in the figure, the slightly different images of the apple are repeated to degrade the quality of the integrated image severely. In Fig. 9(b), the integrated image is located at 59 mm distance from the lens array and the gap is set to 25 mm to locate the central depth plane at 183 mm. In this case, the parts of the integrated image were cut and the entire shape was distorted severely. These results mean that if the central depth plane is formed at 59 mm distance from the lens array to obtain the good quality of the integrated image located around there, the integrated image around 183 mm will be distorted like the image shown in Fig. 9(a), and in the opposite case, the integrated image around 59 mm will be like the image in Fig. 9(b). Therefore, the InIm 3D display system that provides only one central depth plane cannot express the depth region wide enough to include the integrated images around both 59 and 183 mm simultaneously.

Figure 10 shows the experimental results obtained by the InIm 3D display system using the proposed mirror barrier array. In Fig. 10(a), the system is set to the state 1, so the integrated image is expressed at the same location as the central depth plane 1, 183 mm from the lens array as explained before. In Fig. 10(b), the system is changed to the state 2, and both the integrated image and the central depth plane are located at 59 mm distant from the lens array. The vertical black lines shown in the experimental results come from the thickness of the elemental mirrors, and those can be eliminated if we adopt the elemental mirrors that are sufficiently thin. These results show that InIm 3D display system adopting the mirror barrier array can display the integrated images of good quality around both 59 and 183 mm by changing the state of the mirror barrier array with the fixed gap g of 25 mm. Therefore, if we change two states of the mirror barrier array rapidly, the central depth plane 1 and 2 can be expressed simultaneously and the expressible region of the InIm 3D display system will be extended over an amount of 124 mm in the direction perpendicular to the lens array.

5 Discussions and conclusions

The primary advantage of our proposed method with the polarization devices is that we can observe 3D images that maintain some level of viewing resolution with a large depth difference without any mechanical moving parts. And the other scheme, utilizing a mirror barrier array, had the advantage of the compact thickness. These systems have more compact structure compared to the scheme using double display devices and a lens array or the scheme that uses a uniaxial crystal plate. In the scheme using polarization devices, real-virtual or real-real (virtual-virtual) 3D images with a large depth difference can be displayed simultaneously by adjusting the distance difference from a beam splitter to a mirror in each arm. Furthermore, the brightness of real and virtual images is similar because two beams in both arms are transmitted and reflected equally. Although the light loss due to the polarization transmission and relay optics is a bottleneck to limit the usefulness, this proposal can be an attractive solution to overcome the problem of depth-limitation in 3D display based on InIm. In the scheme using a mirror barrier array, the large expressible depth range had been obtained by controlling whether the reflection between neighboring mirrors occurs or not. Although the mechanical motion can be a drawback of this scheme, its compact thickness is very attractive.

Acknowledgment

This work was supported by the Next-Generation Information Display R&D Center, one of the 21st Century Frontier R&D Programs funded by the Ministry of Science and Technology of Korea.

References

1 G Lippmann, "La photographie integrale," *Comptes-Rendus* **146**, 446–451 (1908).
2 T Okoshi, *Three-Dimensional Imaging Techniques* (Academic Press, New York, 1976).
3 S A Benton, "Selected Papers on Three-Dimensional Displays," *SPIE Milestone Series, 2001.*
4 N Davies, M McCormick, and L Yang, "Three-dimensional imaging systems: a new development," *Appl Opt* **27**, 4520–4528 (1988).
5 F Okano, H Hoshino, J Arai, and I Yuyama, "Real-time pickup method for a three-dimensional image based on integral photography," *Appl Opt* **36**, No. 7, 1598–1603 (1997).
6 J Arai, F Okano, H Hoshino, and I Yuyama, "Gradient-index lens-array method based on real-time integral photography for three-dimensional images," *Appl Opt* **37**, No. 11, 2034–2045 (1998).
7 L Erdmann and K J Gabriel, "High-resolution digital integral photography by use of a scanning microlens array," *Appl Opt* **40**, No. 31, 5592–5599 (2001).
8 S Jung, J-H Park, H Choi, and B Lee, "Viewing-angle-enhanced integral three-dimensional imaging along all directions without mechanical movement," *Opt Express* **11**, No. 12, 1346–1356 (2003).

9 J-H Park, S Jung, H Choi, and B Lee, "Viewing-angle-enhanced integral imaging by elemental image resizing and elemental lens switching," *Appl Opt* **41**, No. 32, 6875–6883 (2002).
10 B Lee, S Jung, and J-H Park, "Viewing-angle-enhanced integral imaging by lens switching," *Opt Lett* **27**, No. 10, 818–820 (2002).
11 J-H Park, S-W Min, S Jung, and B Lee, "Analysis of viewing parameters for two display methods based on integral photography," *Appl Opt* **40**, No. 29, 5217–5232 (2001).
12 B Lee, S Jung, S-W Min, and J-H Park, "Three-dimensional display by use of integral photography with dynamically variable image planes," *Opt Lett* **26**, No. 19, 1481–1482 (2001).
13 B Lee, S-W Min, and B Javidi, "Theoretical analysis for three-dimensional integral imaging system with double devices," *Appl Opt* **41**, No. 23, 4856–4865 (2002).
14 J-H Park, S Jung, H Choi, and B Lee, "Integral imaging with multiple image planes using a uniaxial crystal plate," *Opt Express* **11**, No. 16, 1862–1875 (2003).



Sungyong Jung received his B.S., M.S., and Ph.D. degrees, all in electrical engineering from Seoul National University, Seoul, Korea, in 1997, 1999, and 2004, respectively. Since 2004, he has been engaged in research and development of 3-D display at Samsung Electronics Co. When the research for this paper was performed, he was with the Seoul National University. His research interests are stereoscopic and autostereoscopic 3-D displays including integral imaging.



Jisoo Hong received his B.S. degree in electrical engineering from Seoul National University, Korea, in 2002. He is currently working toward his M.S. degree in the School of electrical engineering, Seoul National University. His primary research interests are in the areas of three-dimensional imaging and display including integral imaging.



Jae-Hyeung Park received his B.S. and M.S. degrees from the School of Electrical Engineering of Seoul National University, Korea, in 2000 and 2002, respectively. He is currently working toward his Ph.D. degree at the School of Electrical Engineering, Seoul National University. His primary research interests are in the areas of autostereoscopic three-dimensional display including integral imaging.



Yunhee Kim received her B.S. degree in electrical engineering from Seoul National University, Korea in 2003. She is currently working towards her M.S. degree in the School of Electrical Engineering, Seoul National University. Her primary research interests are in the areas of three-dimensional display and near-field optics.



Byoungho Lee received his B.S. and M.S. degrees in 1987 and 1989, respectively, from Seoul National University, Korea, in electronics engineering. He received his Ph.D. degree in 1993 from the University of California at Berkeley in electrical engineering and computer science. In 1994, he joined the faculty of the School of Electrical Engineering, Seoul National University, where he is now an Associate Professor. He is a fellow of SPIE and a senior member of IEEE. He has served as a committee member for various international conferences. He has authored or co-authored 120 international journal papers and more than 170 international conference papers. In 1999, his laboratory was honored as a National Research Laboratory by the Ministry of Science and Technology of Korea. In 2002, he received the Presidential Young Scientist Award of Korea. His research fields are three-dimensional display, optical fiber devices, and hologram applications.